

Adsorption of Cupper (II) ion on heterogeneous surfaces of selected low-cost precursors; an application of isotherm, thermodynamic and kinetic models

Uzoije , Atulegwu .Patrick

Department of Environmental Technology
Federal University of Technology Owerri,
Imo State-Nigeria
Patuzong@yahoo.com.hk

Njoku, P.C.,

Department of Chemistry.
Federal University of Technology Owerri,
Imo State-Nigeria

Okolie, Justus .I

Department of Chemistry.
Federal University of Technology Owerri,
Imo State-Nigeria

Enwereuzo., Uzo

Department of Environmental Technology
Federal University of Technology Owerri,
Imo State-Nigeria

Abstract—Copper ions occur naturally in the environment and also prevalent in the waste from metal smelting industries through which it gets to the environment. Excessive intake of copper results to adverse health effects on plant, animals and humans. The present study therefore studied the Adsorption of Cupper (II) ion on three activated bio-adsorbents; Unripe plantain peel, pineapple peel and commercial activated carbon. The activated carbons were characterized for surface morphology and functional groups for removal of Cupper (II) ion from aqueous solution. Batch process was adopted to study the time, temperature effect and isotherm equilibrium of Cupper (II) ion on. Adsorption of Cupper (II) ion on the three adsorbents got to equilibrium at between 80-100 minutes. Adsorption capacity of the three adsorbent was in this order at all temperature values; Unripe plantain peel greater than pineapple peel and greater than commercial activated carbon. Adsorption of Cupper ion increased with temperature, adsorption got to its plateau at 45°C and began to decrease. Langumuir-freunlich and Dubini-Radushkevich models were applied to analyze the Isotherm data. Langumuir-freunlich described the data better than Dubini-Radushkevich. Also, Pseudo-first-order, pseudo-second-order, and intra-particle diffusion models were applied to test the kinetic data, pseudo-second-order fitted the data better than pseudo-first order. Pore-pore particle diffusion was observed to be the controlling step. Endothermic and non- spontaneous processes characterized Cupper ion adsorption on the three adsorbents .

Keywords—*Adsorbent, Adsorption, Cupper Models, Thermodynamics, Kinetics, Equilibrium.*

1.0 Introduction

The advent of industrialization and urbanization accompanied negative twist in the ecosystem due to

waste generalization and discharge. Wastes from both large and small scale companies released into the environments have large amounts of heavy metals [1]. Aside direct discharge from the industries, heavy metals get into river bodies through surface run-off and overland flow [2], [3]. The recalcitrant nature of these metals makes them readily available for accumulation in the tissues of plant, animals and humans [4]. Also, the sparingly soluble disposition of heavy metals makes them highly susceptible to adsorption onto the soil matrix during surface run-off infiltration [1]. Heavy metal adsorptions on soil surface could portend danger to the crops and in turn to animals and humans through food-chain [5]. Most heavy metals are carcinogenic on aquatic life and humans [6]. Several treatment approaches have been adopted to reduce the concentration of heavy metals in wastewaters to barest minimum. Methods such as reverse osmosis, membrane systems, ion-exchange, coagulation etc. [7][8],[9], [10] and [11] yielded meaningful results but their apparent Non-affordability with respect to high cost of production, complex and sophistication in operation necessitated further researches on the use of natural adsorbents harnessed from waste materials . The simple technique and simple instruments involve in producing this low cost adsorbent, make adsorption process easy to operate and also a popular technology in water and wastewater management outfits [11]. The porous structure of the activated carbon material which consists of interconnected micro, meso and macro-pores with high surface area makes it an excellent adsorbent for pollutant removal [12]. (Fidelis et al 2013[13], Hasan et al 2008,[14] Wang and Chen 2009[15] and Uzoije et al 2014)[16] applied the use of activated coconut shell, , Masa tree leaf powder and palm kernel shell to remove Pb, Cd, Zn, Fe²⁺/Fe³⁺ respectively from wastewater. In recent past, activated carbon of unripe plantain peel (UPP) and pineapple peel (PP) have been robustly applied to remove phenol, Chromium ion, Pb²⁺ and Cd²⁺ from the

wastewater with an impressive removal result [17] and [18]. Unripe plantain peel has successfully been applied in activated form to remove zinc ion from wastewater [19]. Ninety five percent efficiency was achieved by banana peel biomass sorption of Cu (II) ion from wastewater [20]

The present study is an attempt to compare Cu²⁺ ion removal efficiency from wastewater by Unripe plantain peel (UPP), pineapple peel (PP) and commercial activated carbon.(CAC). UPP and PP Constitute large proportions of solid waste in dump sites especially in this part of the world where they are ubiquitous. Given their high nutritional values the rate of consumption of unripe plantain and pineapple is high. Consequently, their peels are everywhere and therefore constitute substantial quantity of solid waste in dump sites. Copper reaches the environment through natural process and also through mining operations, acidic water and corroding copper pipes [21]. At concentration range of 1.0 to 5.0 ppm, copper can cause staining, corrosive effects and toxicity to plant, animals and humans [22]. Excessive copper in human system may result to capillary damage; hepatic and renal damage [22] and [23]. In the blood, copper causes damage to lipids, proteins and DNA [1]. Fishes also suffer severe damage in the gills, liver and kidney due to excessive copper intake [24]. In these regards, it is expedient that copper polluted wastewater be treated prior to discharge into receiving environmental media such as water and land. This study will therefore carry out removal of Cu²⁺ from aqueous solution using adsorption techniques with convenient and economically viable adsorbents, UPP,ACA and PP. During the adsorption process, the sorption isotherms and kinetics will be measured experimentally and the trend of adsorption will be studied using classical isotherm, thermodynamic and Kinetic models.

2.0 MATERIALS AND METHODS

2.1 PREPARATION AND CHARACTERIZATION OF THE ACTIVATED ADSORBENTS

Unripe plantain peels and pineapple peels were collected from fruit sellers in the Owerri. The plantain and pineapple peels were washed first with tap water to remove dirt and mud and finally washed with distilled water. After washing, they were sun-dried for about two weeks, before grinding with a ball mill. The ground plantain peels and pineapple peels were sieved with a sieve of mesh sizes 1.00mm – 1.18mm. The precursor obtained was washed with distilled water to remove surface bound impurities and dried in the oven at 100°C for 24 hours. 200g of each sample was mixed with 400ml of 1 M H₃PO₄ until the mixture formed a paste. The paste was dried in the oven at 100°C for 24hours. After drying in the oven, the sample was transferred to a crucible and pyrolysed in a muffle furnace at 300°C for 2hours. The pyrolysed material was finally washed with distilled water to bring its pH to 7 and oven dried for 24hours to get a plantain peel and pineapple peel based carbon. The

activated unripe plantain peel pineapple peel and commercial activated carbon were characterized by Fourier Transform Infra-red Spectrophotometer (FTIR) and Scanning Electron Microscope (SEM)

2.2 DETERMINATION OF SURFACE CHEMISTRY

The surface functional groups of the activated carbon were estimated by Fourier Transform Infra-red Spectrophotometer (FTIR). FTIR of the different samples was recorded within 500cm⁻¹-4500cm⁻¹. Samples of 0.1 g was mixed with 1 g of KBr, spectroscopy grade (Merk, Darmstadt, Germany), in a mortar. Part of this mix was introduced in a cell connected to a piston of a hydraulic pump giving a compression pressure of 15 kPa / cm². The mix was converted to a solid disc which was placed in an oven at 105 C for 4 hours to prevent any interference with any existing water vapor or carbon dioxide molecules. Then it was transferred to the FTIR analyzer and a corresponding chromatogram was obtained showing the wave lengths of different functional groups in the sample.

2.3 MICROSCOPY

The surface morphology of the activated carbon samples was analyzed by Scanning Electron Microscopy (SEM). Surface topographical information was obtained by a surface morphological study in the field electron Hitachi S-5200 Scanning Electron Microscope. Well ground carbon samples were placed on a sample stub with the aid of a graphite conductive adhesive paste before being firmly loaded on a cylindrical rod which serves as the sample holder. The rod was thereafter placed in the analysis chamber of the SEM which remains under vacuum all through the analysis. When excited primary beam of electrons from the light source struck the samples , various secondary electrons from the sample surface were emitted which were characteristic of each of the samples. Various secondary electron detectors attracted the scattered electrons, and the signals were used

2.4 EQUILIBRIUM ADSORPTION STUDIES;

The activated UPP adsorbent of 0.1g was degassed under vacuum using 10cm³ of distilled water. Inside the solution, 50ml of determined concentration of the adsorbate were added and stirred with a magnetic stirrer. After attaining adsorption equilibrium, certain amount of the solution was decanted and spectrophotometric method was adopted to determine the amount of adsorbate remaining in the solution at equilibrium. The adsorption equilibrium process was repeated for eight different adsorbate concentrations and repeated for PP and ACA adsorbents at 20, 45, 60, 75 and 85°C temperature levels. The adsorbed amount of Cu²⁺ was calculated from the following mass balanced equation;

$$q_{eq} = \left(\frac{C_0 - C_{eq}}{M} \right) V \quad (1)$$

To Analysis the experimental data, the linear form of the following models were considered; Langmuir, Dubini-Radushkevich and Langmuir-Fruehlich models respectively. Langmuir-Fruehlich(LF) model was chosen taking into account the energetic heterogeneity nature of solid phase[25].

Langmuir model quantifies the adsorption performance of adsorbent with a monolayer adsorption [26]. This implies that the adsorption layer is one layer in thickness. Langmuir favours a situation where each site has definite affinity for adsorption, hence homogenous adsorption. Langmuir is expressed as

$$Q_{eq} = \frac{KC_{eq}}{1+KC_{eq}} \quad (2)$$

$$\text{If } Q_{eq} = \frac{q_{eq}}{a_m} \quad (3)$$

Equation 3 is the relative adsorption coverage of the adsorbents by the solute. a_m explains the mono layer capacity or the adsorption capacity.

Substituting equation 3 in 2 and rearranging it to get a linear form, gives

$$\frac{1}{q_{eq}} = \frac{1}{a_m} + \frac{1}{Ka_m C_{eq}} \quad (4)$$

Dubini-Radushkevich model expresses the adsorption mechanism with energy distribution onto a heterogeneous surface [12] and [27], the model is expressed as

$$q_{eq} = q_s \exp(-K_{ad} \varepsilon^2) \quad (5)$$

The linear form of equation 5 is expressed as follows

$$\ln q_{eq} = \ln q_s - K_{ad} \varepsilon^2 \quad (6)$$

$$\text{But } \varepsilon^2 = RT \ln \left[1 + \frac{1}{C_e} \right] \quad (7)$$

Plot of $\ln q_{eq}$ vs ε^2 gives a linear curve in which K_{ad} was determined as slope and q_s as intercept.

Langmuire-Frundlich model was also used for the analysis of the experimental data is expressed as;

$$Q_{eq} = \frac{(KC_{eq})^m}{1+(KC_{eq})^m} \quad (8)$$

Equation 8 was linearized by taking the natural log of both sides of the equation and is expressed as follows;

$$\ln \left[\frac{Q_{eq}}{(1-Q_{eq})} \right] = m \ln K + m \ln C_{eq} \quad (9)$$

where m represents LF coefficient and explain the heterogeneity of the surface adsorbent. The heterogeneity parameter, m characterizes the shape of adsorption energy distribution function and is put in the following range [26] [28]). The range of heterogeneity parameter is expressed as follows. $0 < m \leq 1$. K describes the position of energy distribution functions.

2.5 KINETIC STUDIES;

The kinetic study was carried out by performing an experiment involving UPP adsorbent and concentration of the adsorbate(Cu^{2+}) solution mixed in a 500ml glass flask and stirred with a magnetic stirrer. At a definite time interval, certain amount of the sample was removed, analyzed and calculated for the solute concentration onto the adsorbent and that in the solution. The experiment was repeated with PP and ACA types of the adsorbent and at various temperature ranges of 20, 45, 60, 75 and 85 degrees centigrade. The data obtained were analyzed using pseudo- first and second other kinetic models. intraparticle diffusion models were also applied to further study the kinetic behavior of the adsorption process. Pseudo-first order models with respect to concentration and adsorption were expressed as;

$$\frac{dC}{dt} = -K_1(C - C_{eq}) \quad (10a)$$

$$\frac{dC}{dt} = K_1(a_{eq} - a) \quad (10b)$$

respectively

Integrated form of the equations referred to as lagergren equations were shown respectively as

$$\ln(C - C_{eq}) = \ln(C_0 - C_{eq}) - K_1 t \quad (11a)$$

$$\ln(a_{eq} - a) = \ln(a_{eq} - K_1) \quad (11b)$$

Also applied in this study was the most widely used equilibrium dependent pseudo-second order kinetic equation expressed as

$$\frac{da}{dt} = K_2(a_{eq} - a)^2 \quad (12a)$$

Integration of equation of 12a is expressed as follows

$$\frac{t}{a} = \frac{1}{K_2 a_{eq}^2} + \frac{t}{a_{eq}} \quad (12b)$$

Migration of solute in a solution into the adsorbent takes effect through three distinct steps. These are ; migration of the solute from aqueous solution to adsorbent boundary surface, diffusion of solute in the adsorbent pore, which is usually a slow process, and intra-particle diffusion of solute particles. In adsorption processes, transport of solute particles observe all these steps with at least one step controlling the process. The intra-particle diffusion was expressed in the following equation;

$$q_t = K_p t^{0.5} \quad (13a)$$

$$\text{Where } K_p = \frac{6q_e}{R} \sqrt{\frac{D}{\pi}} \quad (13b)$$

If the rate determining step of the sorption process is intra-particle diffusion, the linear plot of q_t vs $t^{0.5}$ must pass through the origin with K_p representing the slope.

Also, the liquid film diffusion model describes the transport of solute in aqueous solution to the adsorbent surface boundary is expressed as

$$F = 1 - \frac{6}{\pi^2} \exp(-\beta t) \quad (14a)$$

The natural log and rearrangement of equation 14a is represented as

$$\ln(1 - F) = 0.4977 + (-\beta t) \quad (14b)$$

If $F = \frac{q}{q_e}$ and is substituted into equation 14b the model becomes

$$\ln\left(1 - \frac{q}{q_e}\right) = 0.4977 + (-\beta t) \quad (14c)$$

Rearrangement of equation 14c, expressed βt as follows;

$$\beta t = -0.4977 - \ln\left(1 - \frac{q}{q_e}\right) \quad (14d)$$

If the computed values of βt are plotted with time (t) and the curve passes through the origin, then the sorption process is film diffusion controlled.

2.6 THERMODYNAMICS

Temperature is an important factor in adsorption processes. It stimulates the adsorbent properties such as the functional group, surface morphology and molecules [29]. It also stimulates the adsorbates by way of raising their potentials for effective adsorption [12], [25] and [16]. All these observations are link to thermo- dynamism of an adsorption process. This segment of the study therefore examined the temperature effect on thermodynamic properties of Cu (II) ion adsorption process onto the adsorbents under study. In the light of this, data collected at different temperature values were used to calculate the Gibb free energy (ΔG^0), enthalpy (ΔH), and entropy (ΔS)

The Gibb free energy or free energy of adsorption was calculated with the following equation;

$$\Delta G^0 = -RT \ln K_a \quad (15)$$

Where R is the universal gas constant (8.314J/mole/°K), T (Absolute temperature °K) and K_a represents the binding Langmuir constant.

Enthalpy of adsorption is the binding energy between the solvent and the adsorbent with solute, and is evaluated graphically by calculating the slope of $\ln K$ VS $\frac{1}{T}$ derived from the following equation;

$$\ln K = \frac{\Delta H}{RT} + constant \quad (16)$$

Entropy of adsorption was obtained with the equation below

$$\Delta G = \Delta H - T\Delta S \quad (17)$$

3.0 RESULTS AND DISCUSSIONS

Figs 1-3 show FTIR spectra for the adsorbents. Variations of bands were observed on the adsorbent used for this study. The figures show bands of varying peaks with absorption band medium for UPP, PP and CAC identified as 3300 cm^{-1} -383.88 cm^{-1} , 3800 cm^{-1} -421.46 cm^{-1} and 3900 cm^{-1} – 361.93 cm^{-1} respectively. The broad bands of 3900, 3800 and 3300 for the respective adsorbent indicate hydroxyl stretching. Also prominent in the band spectra for the adsorbents

are absorption band media ranges of 29031.50-2283.79, 29947.33-2275.11 and 2400 for CAC, PP and UPP respectively.

These band ranges indicate CH_2 stretching. A medium absorption band ranges of 1725.38-1104.28, 1746.60-1400 and 1742-11.84 cm^{-1} for UPP, PP and CAC respectively, representing aromatic C=C Stretching was also identified

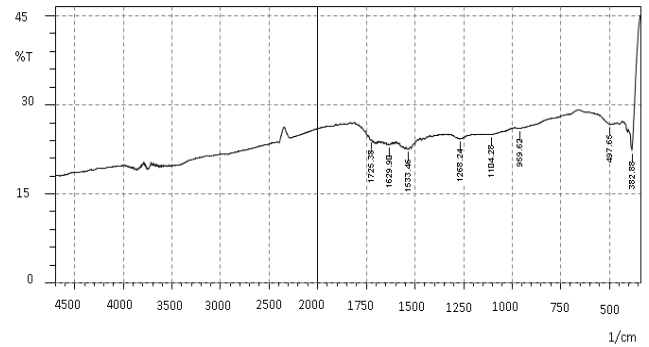


Fig 1: FTIR Analysis of UPPAC.

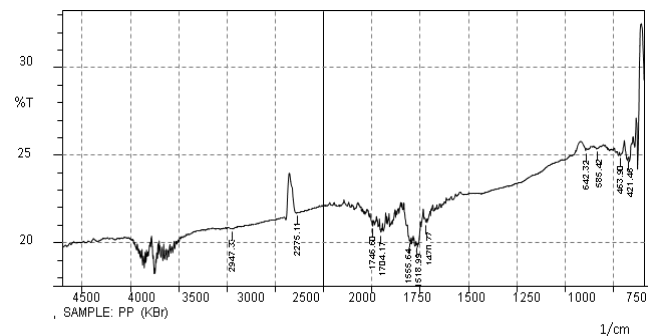


Fig 2 . FTIR Analysis of PPAC

Strongest broad bands were observed in CAC spectrum followed by PP with UPP having the weakest bands. Relationships between hydroxyl functional group and adsorption of Cu^{2+} ion were observed. PP and CAC adsorbents where hydroxyl functional groups were present in large amount, showed high adsorption capacity for Cu^{2+} ion when compared with UPP adsorbent. Physical morphology study of the adsorbent surfaces showed texture with heterogeneous surfaces and variety of pore sizes and cavities as shown on figures4-6 .Pores and cavities are responsible for increase in surface area, adsorption capacities and efficiencies [12] and [30]

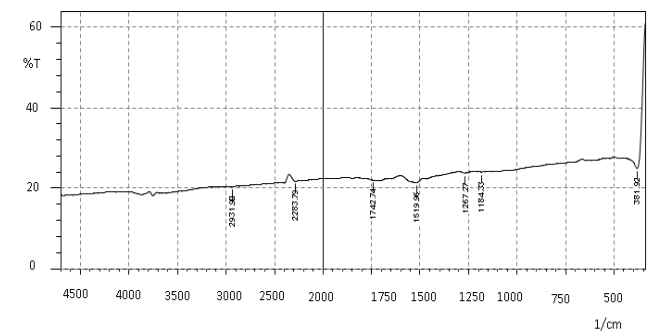


Fig. 3: FTIR Analysis of CAC

It was observed that PP and ACA have higher number of pores and cavities than UPP. Consequently, Cu^{2+} ion adsorption on various adsorbents (PP, ACA and UPP) vary accordingly. Adsorption was high on PP and ACA, apparently due to high surface area and pore sizes.

The adsorption equilibrium study data were analyzed with Dubini-Radushkevich and Langmuir-Fruehlich models expressed as equations 6 and 9 respectively. From the analysis, Langmuir-Fruehlich(9) represented the data better than the Dubini-Radushkevich(6) model(see figs 7 and 8 and table1).Correlation coefficient values(R^2) in all the systems were between 0.80 – 0.98 .

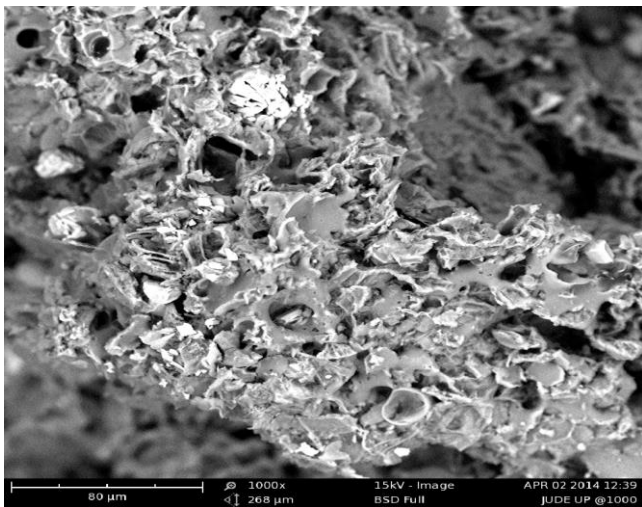


Fig. 4 : SEM image of UPPAC at 1000x

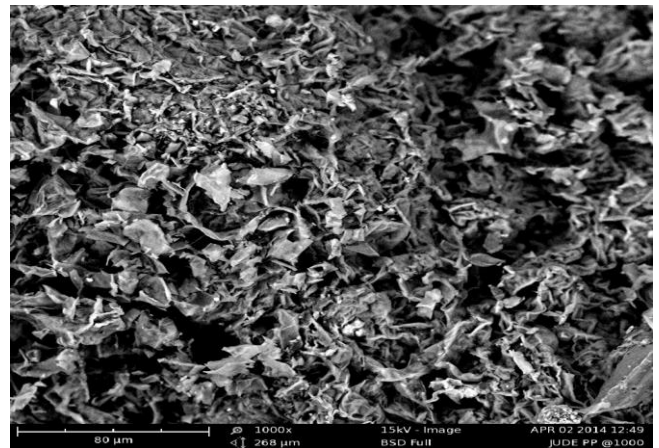


Fig. 5: SEM image of PPAC at 1000x

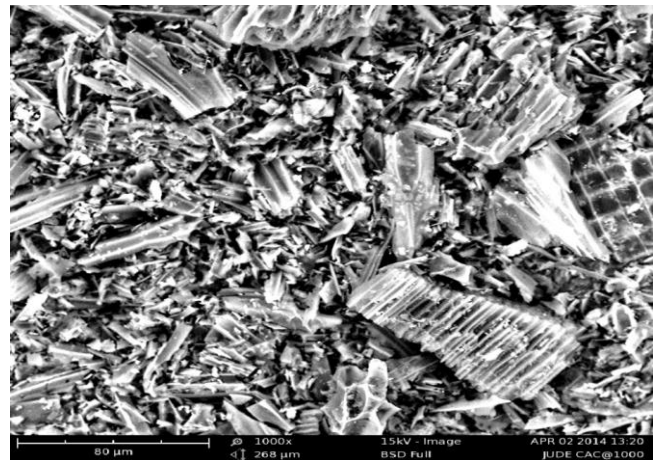


Fig. 6: SEM image of CAC at 1000x

Parameters of equation (9) obtained from line fitting procedure at different adsorption systems were also shown on table1.

Table 1 ; Calculated Langmuir-freundlich and Dubinin-Radushkevich isotherm fitting parameters using fitting curves and adsorption of Cu(II) ions on UPP, PP, and CAC Carbons from aqueous solution.

Temp.(Oc)	Langmuir-Freundlich parameters						Dubinin-Radushkevich parameters		
	Adsorbent	A_m	M	K	R^2	\emptyset	$q_s(\text{mg/g})$	$K_{ad}(\text{mol}^2/\text{KJ}^2)$	R^2
20	Cu(II)/UPP	81.97	0.878	0.0084	0.814	0.002	2134.76	196.5	0.543
	Cu(II)PP	142.19	0.865	0.0165	0.839	0.0047	2543.22	1865.76	0.748
	Cu(II)CAC	229.41	0.845	0.024	0.813	0.0068	3061.76	1908	0.387
45	Cu(II)/UPP	214.12	0.89	0.003	0.933	0.0008	2776.3	1571.7	0.91
	Cu(II)PP	384.75	0.867	0.01	0.956	0.0027	6223.6	315.9	0.142
	Cu(II)CAC	224.39	0.75	0.02	0.936	0.009	2237	2566.1	0.469
60	Cu(II)/UPP	43.29	0.95	0.011	0.964	0.004	3260.7	1269.4	0.767
	Cu(II)PP	176.92	0.91	0.019	0.908	0.003	2737.5	1826.3	0.922
	Cu(II)CAC	162.5	0.894	0.01	0.913	0.0023	2529.2	1984.8	0.925
75	Cu(II)/UPP	25.84	1.018	0.036	0.986	0.0057	2951.3	1246.2	0.877
	Cu(II)PP	100	0.723	0.001	0.86	0.0002	3425.6	1362.9	0.874
	Cu(II)CAC	90.8	0.952	0.0022	0.889	0.0005	3040.2	1642	0.875
85	Cu(II)/UPP	18.98	1.107	0.0565	0.96	0.0066	3205.5	953.12	0.849
	Cu(II)PP	73.64	1.014	0.0095	0.808	0.0015	3745.7	1162.7	0.789
	Cu(II)CAC	155.56	0.999	0.0018	0.82	0.0003	3448	1311.6	0.825

All the adsorbents under study showed strong heterogeneity effects, this is evident on the low values of heterogeneity parameters; m obtained for UPP, PP and ACA. Surface heterogeneity of adsorbent is a measure of adsorption capacity [24]. An adsorption surface becomes more heterogeneous as m value tends to zero [22] and [32]. Some studies also confirmed chemisorption adsorption process with m values below unity as it was the case in most adsorption systems of this study [33] and [26]. m values for adsorption systems of PP and ACA were lower than that of UPP in all the temperature values, suggesting high adsorption of Cu^{2+} . This was corroborated by adsorption capacity values; a_m , of all the systems. The a_m values for PP and ACA were higher than that of UPP. This implied that UPP having lower surface heterogeneity (high m values) has less adsorption capacity. The small pore sizes prominent in UPP adsorbent which is characterized by low surface heterogeneity created bottle-necks for effective uptake of Cu^{2+} on the adsorbent. The apparent low adsorption capacity observed in UPP could also be as a result of too large Cu^{2+} molecules joisting for limited amounts of adsorbent pores [34] and [35]. This condition buttressed earlier observation which had it that limited adsorption active sites retard effective adsorption [36]. Equilibrium constants; K describes the position of energy distribution functions [34]. In this study, K varies appreciably with adsorption systems. The study showed higher K values in PP and ACA adsorption systems than that of UPP, implying more adsorption energy of PP and ACA and consequent more adsorption capacity. Apart from adsorbent configurations (surface area, functional groups and pore sizes) earlier discussed, temperature has apparent effects on the adsorption capacity of the adsorbents used in this study. From the results shown on table 1, the adsorption capacity varied with changes in temperature values. Adsorption capacity increased at temperature values of 20 and 45 but started declining at temperature range of 60 – 80.

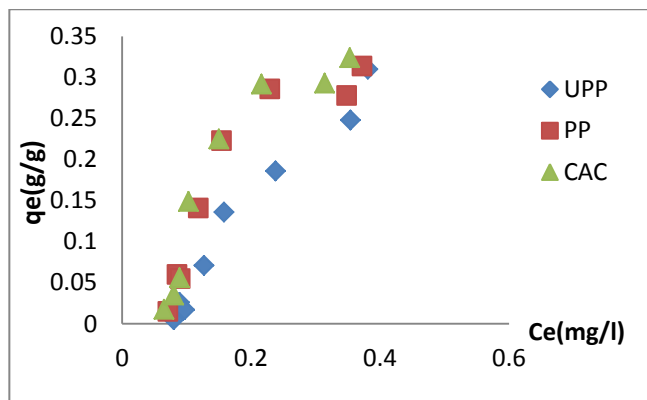


Fig 7; Adsorption isotherm of Cu (II) on UPP, PP and CAC at 85°C with pH of 6

The prevailing trend could be attributed to increase in mobility of Cu^{2+} ion towards the adsorbent and decrease in the retarding forces of diffusing Cu^{2+} ion, thereby fostering effective adsorption as the

temperature values increased from 20°C to 45°C. Increase in temperature could also lead to easy penetration of adsorbent structure thereby overcoming activation energy barrier with concomitant enhancement of intra-particle migration, resulting to increase in adsorption capacity of the adsorbents at elevated temperature [33], [37] and [38]). Also, enlargement of adsorbent pore sizes increasing with temperature, could be linked to the present observation [39] and [40]. Increase in solubility of the Cu^{2+} ion [25] and oscillation energy of Cu^{2+} ion [41], [12] leading to decrease in adsorption capacity and desorption of the $\text{Cu}(\text{II})$ molecules at higher temperature respectively could also lead to the reverse trend of adsorption process observed in this study.

From the Kinetic analysis, quantity of Cu^{2+} ion adsorbed increased with time until the adsorption process reached a plateau at 100 minutes and, no appreciable adsorption was observed thereafter. See fig 9.

The initial fast Progressive Cu^{2+} ion adsorption process observed in fig 9 could be as a result of availability of non-used binding adsorption sites at the initial stage [42] and [12]. Later adsorptions got to equilibrium when the sites had been used up.

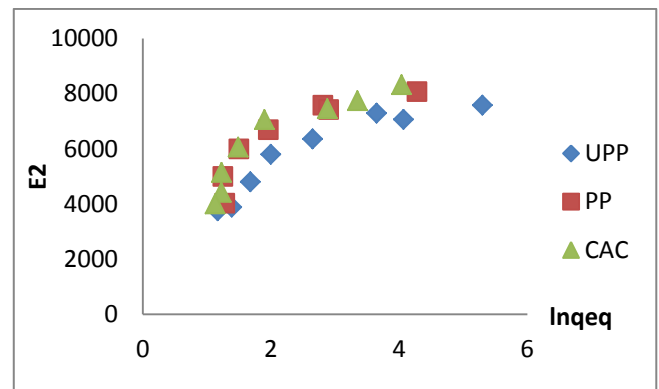


Fig 8 Dubini-Radushkevich Adsorption isotherm of Cu (II) on UPP, PP and CAC at 85°C with pH of 6

Pseudo first and second order kinetic models showed straight line curves of $\log(a_{eq} - a)$ Vs t and $\frac{t}{a}$ Vs t at time intervals and various adsorption systems respectively (see figures 11 and 10). Comparing the two kinetic models, pseudo second order described the kinetic study better than pseudo first with their correlation co-efficient (R^2) at 0.88-0.98 and 0.993-0.996 respectively. The kinetic rate constants, K_1 and K_2 determined from the slope and intercept of pseudo First and second order curves respectively, were shown on table 2. K_2 values were close to unity which confirmed chemisorption- controlled- process [20], [43], [44] and [2]. To further study kinetic behaviours of the adsorption process, classical pore diffusion models were applied. These mathematical models distinguished between film diffusion (equation 13a) and intra-particle diffusion (equation 14d) in an adsorption process [12]

In this study, curve of the plot of q_t vs $t^{0.5}$ as shown by figure12, producing a non-straight curve without passing through the origin, implies that intra-particle diffusion phenomena is not the rate controlling step. Particles of Cu^{2+} ion experiencing some resistance actualize intra-particle diffusion could be attributed to micro-pore structures of the adsorbents. The adsorbents used for this study have different pore configurations with respect to sizes as earlier observed. PP and ACA have larger pore-size than UPP and the intra-particle diffusion rate constant q_p varied accordingly (see table2). Previous researchers observed that big molecules of the adsorbate slow down intra-particle diffusion [45] and [46]. Also, for physical adsorption to occur in the pores, the pores must be large enough for the molecules to enter [47] and [48]. In the same vain, plot of βt vs t (see fig13) was made and a linear curve was also produced with non-zero intercept, this suggested that film diffusion did not equally play significant role in the adsorption process of Cu^{2+} onto the adsorbents under study.

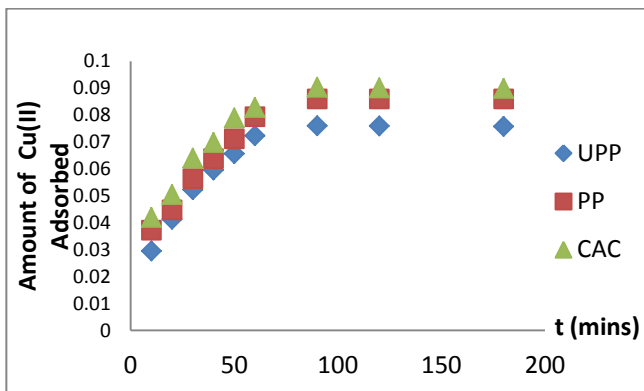


Fig 9 Adsorption trend curves of Cu(II) at Initial concentration of 200mg/l and adsorbent mass of .1g on various UPP,PP and CAC

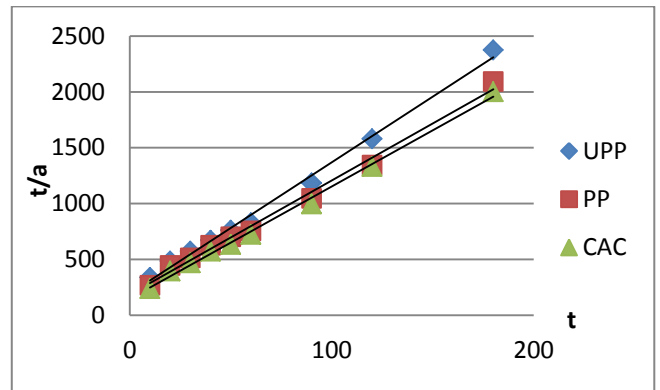


Fig 10 Pseudo-second order plot of the sorption kintetics of Cu(II) of UPP, PP and CAC

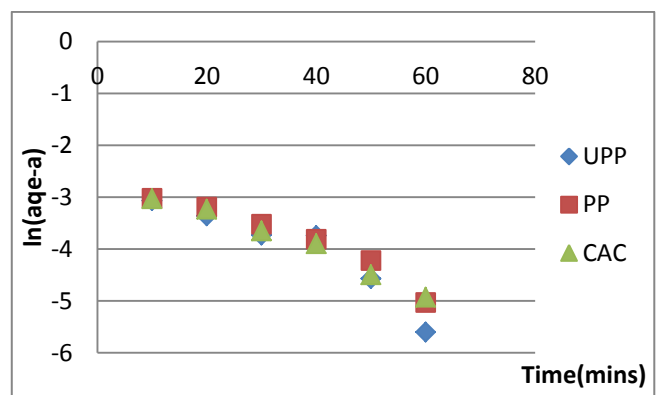


Fig 11 pseudo-first order plot of the sorption kinetics of Cu (II) of UPP, PP and CAC

Table 2; Values of the Kinetic and thermodynamic Parameters

Adsorbents/adsorbate	First order kinetic parameters			Second order			Diffusion models	
	K1	R2	aeq(mg/g)	K1	R2	aeq(mg/g)	Kp	R2
Cu(II)/UPP	0.0466	0.8822	10.82	0.061	0.9942	85.03	10.4	0.8893
Cu(II)PP	0.0384	0.9375	11.65	0.055	0.9925	97.6	12.34	0.8251
Cu(II)CAC	0.0387	0.9782	12.41	0.07	0.9959	99.43	13.29	0.9113
Thermodynamic parameters								
Adsorbent/Adsorbate	temp(°C)	ΔG	ΔH	ΔS				
Cu(II)/UPP	20	316.68	932.415	2.12				
	45	660.96		0.83				
	60	1010.52		0.24				
	75	1513.18		1.67				
	85	1973.36		2.91				
Cu(II)/PP	20	3483.48	1178.51	0.01				
	45	568.43		1.92				
	60	11295.73		30.38				
	75	20426.5		55.31				
	85	23632.71		62.72				
Cu(II)/CAC	20	9549.13	554.23	30.7				
	45	10337.46		30.77				
	60	13593.64		39.16				
	75	17706.83		49.29				
	85	20775.36		56.48				

Deviation of the line curves from the origin could be attributed to differences in mass transfer rate [49], [50]

Values of thermodynamics parameters;

Gibb free energy(ΔG), *enthalpy heat of adsorption*

(ΔH) and *entropy*(ΔS) were summarized in table 2 . Positive values of (ΔG) and their increase with temperature is an indicative of the fact that the adsorption process was not spontaneous even at higher temperature. Adsorption of Cu^{2+} on various systems was an endothermic process, given the positive ΔH values. Also, positive values of ΔS confirmed good adsorption of Cu^{2+} on the adsorption systems.

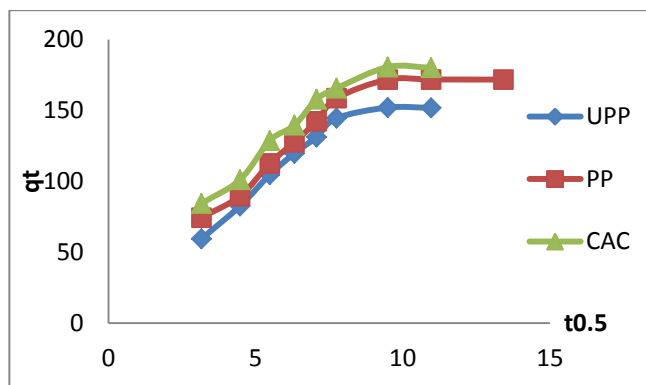


Fig 12 plot of qt Vs $t_{0.5}$ for $Cu(II)$ ion uptake by various adsorbents

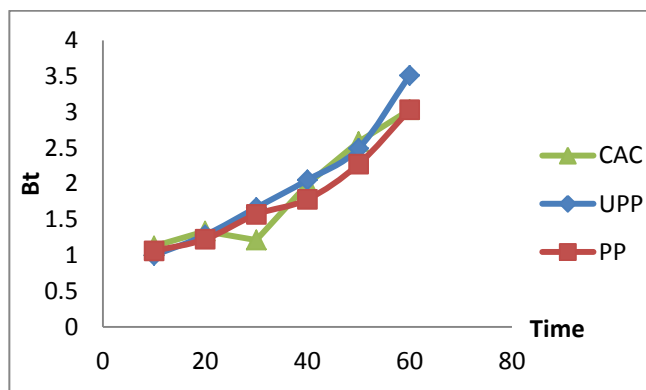


Fig 13 plot of βt Vs time for $Cu(II)$ ion uptake by various adsorbents

Conclusions

Three adsorbents (UPP, PP and CAC) of varying heterogeneity pore sizes and cavities were used for this study. UPP has the least number of pore sizes followed by PP and CAC has the highest number of pore sizes. Adsorption capacity of Cu^{2+} on these adsorbents varied accordingly. Adsorption of Cu^{2+} ions was at equilibrium at between 80 to 100 minutes on the three adsorbents under study. Adsorptions of Cu^{2+} on the three adsorbents were progressive with temperature until at $80^{\circ}C$ when adsorption retrogressed with temperature. Freunlich-Langumiur model better described the equilibrium isotherm study. Second order kinetic model gave a better fit to the

data generated from the kinetic behaviour of Cu^{2+} on the adsorbents. Pore-pore diffusion of Cu^{2+} ion within the adsorbents was the rate controlling step. The calculated thermodynamic parameters indicated that Cu^{2+} ion adsorption on the adsorbents is non-spontaneous and endothermic.

Acknowledgment

The research work was co-sponsored by the authors. We remain grateful to ministry of science and technology Uyo, akwa-ibom state, Nigeria and management of federal university of technology Owerri Nigeria for making their laboratories available for adsorbate characterization and activation of the adsorbents respectively.

REFERENCES.

- [1] George, A,B, 2010, Cu toxicity in the general population. Clinical neurophysiology 121(4) 459-460
- [2]Jalall and rowell the role of calcite and gypsum in the leaching of potassium in a sandy soil. Experimental agriculture 39;379-394. 2003
- [3] Nasim,A.K, Shaliza, I and piarakaram,s. 2004; elimination of heavy metals from wastewater using agricultural waste as adsorbents; Malaysian journal of Sci. 23;43-51
- [4] Malakootian M, Nouri,T and Hossaini, H (2009). Removal of heavy metals from paint industry's wastewater using Leca as an available adsorbents. Int.J. Env.Sci Tech 6(2)183-190.
- [5] Selim, H.M and Amacher,M.C, 1997; reactivity and transport of Heavy Metals in soils CRC/Lewis publishers, Boca Raton. 23(3)321-341
- [6] Gregory , A.R. , Eliot, S K and P. Ames. Testing of direct black 3 parallel carcinogenicity. Journal of applied toxicology. 1, 303-313 1999.
- [7] Forgacs, E, Cserhati, T, . Removal of synthetic dye from wastewater; a review. The environment 30(2004) 953-971
- [8] Robinson , T, McMullan, R Marchant, Nigain, P; Remediation of dye in textile effluent a critical view on current treatment techniques with a proposed alternative biomass, technology 77(2011)247-255
- [9] Gupta, V.K, Mittal, A, Krishnan, L, Gajba,V. Adsorption kinetics and column operations for the removal and recovery of malecite green from wastewater using bottom ash, sep. purify. technology 40(2004)87-96
- [10]Yang C.L, McGarrahan, J, Electron-chemical coagulation for textile effluent decolorization. J Hazardous Materials 117(2005) 171-178.
- [11]Noll, K.E, Vassillios, G, Sttou,W. Adsorption technology for Air and water pollution control lewis publishers Chelsea MI USA 1992

- [12] Derylo-Marczewski, A.D., Blanchind, M, Marczevske, A.W, Swiatkoweri, A, Tarasiuk, B. Adsorption selected herbicides from aqueous solution on activated carbon. *J. Them Anal calorim* 100;785-794 2010.
- [13] Fidelis chigondy, tensty Nyembuya and Marko chingodo; removal of Zn(II) ions from aqueous solution using Msasa tree. *Equilibrium study. J of Asian scientific research*; 2013 3(2)140-150
- [14] Hasim, S.H, sing, K.K, Prakash, O, Talat, M and Ho, Y.S 2008, removal of Cr(VI) from aqueous solution using agricultural waste maize. *J of hazardous materials* 152(1);356-365
- [15] Wang, J.C and Chen A.P 2009. Bio-sorbents for heavy metal removal. *Biotechnology Advances* 27(2);195-312
- [16] Uzoije, A.P Uche, C.C Ashiegbu, D 2014. Analysis of Thermodynamics, kinetics and equilibrium isotherm on Fe^{3+}/Fe^{2+} Adsorption onto palm kernel shell activated carbon (PKSAC): A low-Cost adsorbent. *American Chemical Science journal (ACSJ)*
- [17] Idowu, S.O Oni, S.O and Adesumo, A.A. Biosorption of Cr^{2+} from aqueous solution by biomass of plantain peel, residue, *African J. Med phy, Biomedical engineering and science* 2013, 22-27
- [18] Asiagwu, A.K . sorption kinetic of Pb^{2+} and Ca^{2+} in via biomass. *IJRRAS* 13(2)2012.
- [19] Opeolu, B.O and Fatoki, O.S. dynamics of zinc sorption from aqueous solution using plantain peel biomass. *African journal of biotech* 11(8)13194-13201 2012
- [20] Hossain, M.A, Hgo, H.H, Guo, W,S and Nguyen, T.V, Biosorption of Cu(II) ion from water by banana peel based biosorption, experiments and models of adsorption and desorption. *Journals of water sustainability* 2(1) 2012 287-104
- [21] Akinmosin, A., Osinowo, O.O and Oladunjogbe, M.A. Radiogenic component of the Nigerian tarsand deposits. *Earth science resources journal* 13(1);64-73 2009
- [22] Madhava Rao, Ramesh, A, Purna Chandra, Roa, G and Seshiah, K 2006. Removal Cu and cadmium from the aqueous by activated carbon derived from Ceiba pentandra Hulls. *Journal of Hazardous materials* 129(3) 123-129.
- [23] Rarougs, Meniai, A.H, Hebovine, M.B 2005,. Experimental study of the removal of Cu from aqueous solution by adsorption use sawdust. *Desalination* 185(1)3 483-490
- [24] Van Genderen, E.L., Ryan, A.C., Tomasso., J.R., Klaire, S.J 2005. EVALUATION OF AXUTE Cu toxicity to larval fathead Minnows (pimephales promelas) in soft surface waters . *environmental toxicology and chemistry* 24(2)408-414
- [25] Adam W.M, Anna, D and Agata, S. adsorption and desorption in kinetic of Benzene Derivatives on meso-porous carbons. *Adsorption*(2013)19;391-406
- [26] Foo, T.Y and B.A Hameed. . Insight into modeling of adsorption isotherm systems. *Chemical engineering journals*.156(2010)2-10
- [27] Goswami, S and Ghosh, U.C, . Studies on adsorption behavior of Cr(VI) onto synthetic hydrous stannic oxide water SA. 31, 44 57-602 2005.
- [28] Rudzinski, W, Penezzyk, T . Kinetic of isothermal adsorption on energetically heterogeneous solid surface; a new theoretical desorption based interfacial transport. *J. Phy Chem B* 104, 9149-9162
- [29] Chinagombe, P, Ssaha, B, Wakaman, R.J' Effects of surface modification of an engineered activated carbon on the sorption of 2,4 dichlorophenoxy acetic acid and benzoic acid from water. *J Colloid interfacial sci.* 2006;297;434-442.
- [30] Joseph, Y.F, and Noursh, E. performance, Kinetic and equilibrium in biosorption of anionic of *Saccharomyces cerevisiae* as a low-cost biosorbent. *Turkish J Eng. Evn. Sci.* 37;146-161 2013
- [31] Hamadi, K, Swaminathan, S, Chen, X.D. adsorption of paraquat dichloride from aqueous solution by activated carbon derived from used tires. *J. Hazardous materials* 2004 12 133-141.
- [32] Mustafa, M.R. Adsorption of Mercury, Lead and Cadmium ions on modified activated carbon. *Adsorption science and technology* 1997(156)551-557
- [33] Atiyel, H, Duvnjak, Z. Purification of fructose syrups produced from cane molasses media using ultrafiltration for removal of synthetic and natural organic matter. *Journal of industrial and engineering chemistry*. Vol6 No 6 pp357-364.
- [34] Mittal, A, Krishrian, L and Gupta, V.K. use of waste materials –bottom ash and de-oiled soya as potential adsorbent for the removal of amaranth from aqueous solution *J. hazardous material*.132(34)1432-1441
- [35] Anwar, J, Shafique, U, Waheed, UZ, Salmen, M., Dar, A, Anwar, S (2010). Removal of Pb(II) and Cd(II) from water by adsorption on peels of Banana. *Bioresources Tech.* 101(6), 1752-1755.
- [36] Liu, Y and Shen, L. From Langmuir kinetics to first and second order rate equations for adsorption *Langmuir* 24, 11625-11625.
- [37] Emmanuel A.O, Adewele F.A, and Iyabo, O.O . Removal of Pb^{2+} and d^{2+} ions from wastewaters

- using Kernel Charcoal. Research journal in engineering and applied science 1(5)308-313 2012.
- [38] Mohan,D, and Chander, S, Single component and multi-component adsorption of metal ions by activated carbon colloids surf A. J. Hazardous materials 2001; (177)183-196
- [39] Farah,J.Y, El-Gendy,N.S,, performance and kinetic studies on biosorption of Astrazon Blue Dye by Dried Biomass of Baker's yeast as a low cost biosorption; bioscience Biotech research Asia 4;370-370 2007
- [40] EL-Alla, H.J, EL-Sowsy, K.M, and Hartany,K.A. Kinetic, equilibrium and isotherm of the adsorption of cyanide by MDFSD, Arabian journal of chemistry 2011 4;3 417-450 2011.
- [41]Azizian, S. Kinetic models of sorption; A theoretical analysis. Journal of colloid interface science 276 47-52 (2004)
- [42] Ho, Y.S, Huang,C.T and Huang,H.W. 2006 Equilibrium sorption isotherm for metal ions on tree fern. Process biochemistry 37(2)1421-1430
- 43] Ho, Y,S and Ofomaja, A.E . biosorption thermodynamics of Cd on coconut copra meal as biosorbent. Biochemical Engineering journal 30(20), 117-1232006
- [44] Khambhaty, Y, Mody,K, Basha,S., Jha, B . 2009 Kinetics equilibrium and thermodynamic studies on biosorption of Hexavalent Cr by dead fungal biomass of marine *Asperillus niger* chemical Engineering journal 145(3) 489-495
- [45] Jadhaw, D,N and Vanjare, A.K, Adsorption Kinetic study, removal of Dyestuff effluent using sawdust, polymerized sawdust carbon(II) Indian journal of charcoal technology. 11(1)42-50 2004.
- [46] Ekebafé, L.O, Ekebafé,M.O, Erhuage, G.O, Obaigbo,F.M' Effects of reaction conditions on the uptake of selected heavy metals from aqueous media using composite from renewable materials . American journal of polymer science 2002;2(4)62-72
- [47] His,H.C, Rostan=Abadi,M, Rood, M.J, Chen,S and chana,R 2001. Effects of sulfur impregnated temperature on the properties and mercury adsorption capacity of activated carbon fibers (ACFS). Env, Sci, and tech 35(13)2785-2791.
- [48] Corapcioglu,M.O and Huang,CP. The adsorption of heavy metals onto hydrous activated carbon . water resources. 1987 21;1031-1044
- [49] Mall,I.D, Srivastava,W and Argawel,K. Removal of orange G and methyl violet Dye by adsorption onto Bagasse fly Ash Kinetic study and equilibrium isotherm analysis. Dye and pigments;69, 210-223 2006
- [50] Bhattacharya, A.K, Mandal, S.N and Das S.K 2006 . Adsorption of Zn(II) ions from aqueous solution by using different adsorbents chem. Eng. Journal 123, 43-51.